Derivation of capture cross section from quasielastic excitation function

V.V.Sargsyan[1,2], G.G.Adamian[1], N.V.Antonenko[1], and P.R.S.Gomes[3]

[1]*Joint Institute for Nuclear Research, 141980 Dubna, Russia*
[2]*International Center for Advanced Studies, Yerevan State University, 0025 Yerevan, Armenia*
[3]*Instituto de Fisica, Universidade Federal Fluminense,*
Av. Litorânea, s/n, Niterói, R.J. 24210-340, Brazil
(Dated: April 19, 2013)

The relationship between the quasielastic excitation function and the capture cross section is derived. The quasielastic data is shown to be a useful tool to extract the capture cross sections and the angular momenta of the captured systems for the reactions ^{16}O+^{144,154}Sm,^{208}Pb, ^{20}Ne+^{208}Pb, and ^{32}S+^{90,96}Zr at near and above the Coulomb barrier energies.

I. INTRODUCTION

The partial capture cross section is one of the important ingredients to calculate and predict the production cross sections of exotic and superheavy nuclei in the cold, hot, and sub-barrier astrophysical fusion reactions. Therefore, more experimental and theoretical studies of the capture process are required. There is a relationship between the capture and the quasielastic scattering processes because of the conservation of the reaction flux [1, 2]. Any loss from the quasielastic channel directly contributes to the capture and vise versa. The quasielastic measurements are usually not as complex as the direct capture (fusion) measurements. Thus, the quasielastic data are suited for the extraction of the capture probabilities and of the capture cross sections.

The paper is organized in the following way. In Sec. II we derive the formulas for the extraction of the capture cross section and of the angular momentum of the captured system by employing the experimental quasielastic excitation function. In Sec. III, using these formulas, we extract the capture cross sections and the angular momenta of the captured systems and compare with those of direct measurements. Using the available experimental quasielasic data, we predict the capture cross sections for the cold fusion reactions. In Sec. IV the paper is summarized.

II. RELATIONSHIP BETWEEN CAPTURE AND QUASIELASTIC SCATTERING

The expression

$$P_{qe}(E_{\text{c.m.}}, J) + P_{cap}(E_{\text{c.m.}}, J) = 1 \tag{1}$$

connecting the quasielastic (reflection) P_{qe} and the capture (transmission) P_{cap} probabilities follows from the conservation of the reaction flux [1, 2]. Thus, one can extract the capture probability $P_{cap}(E_{\text{c.m.}}, J = 0)$ at $J = 0$ from the experimental quasielastic probability $P_{qe}(E_{\text{c.m.}}, J = 0)$:

$$P_{cap}(E_{\text{c.m.}}, J = 0) = 1 - P_{qe}(E_{\text{c.m.}}, J = 0) = 1 - d\sigma_{qe}(E_{\text{c.m.}})/d\sigma_{Ru}(E_{\text{c.m.}}). \tag{2}$$

Here, the quasielastic probability [1, 3–5]

$$P_{qe}(E_{\text{c.m.}}, J = 0) = d\sigma_{qe}/d\sigma_{Ru} \tag{3}$$

for angular momentum $J = 0$ is given by the ratio of the quasielastic differential cross section and Rutherford differential cross section at 180 degrees. Further, one can approximate the J dependence of the capture probability $P_{cap}(E_{\text{c.m.}}, J)$ at a given energy $E_{\text{c.m.}}$ by shifting the energy [6]:

$$P_{cap}(E_{\text{c.m.}}, J) \approx P_{cap}(E_{\text{c.m.}} - \frac{\hbar^2 \Lambda}{2\mu R_b^2}, J = 0) = 1 - P_{qe}(E_{\text{c.m.}} - \frac{\hbar^2 \Lambda}{2\mu R_b^2}, J = 0), \tag{4}$$

where $\Lambda = J(J + 1)$, $R_b = R_b(J = 0)$ is the position of the Coulomb barrier at $J = 0$. Then, we extract the capture cross section $\sigma_{cap}(E_{\text{c.m.}})$ from the experimental quasielastic probabilities P_{qe}:

$$\sigma_{cap}(E_{\text{c.m.}}) = \sum_{J=0}^{J_{cr}} \sigma_{\text{cap}}(E_{\text{c.m.}}, J) = \pi \lambdabar^2 \sum_{J=0}^{J_{cr}} (2J + 1)[1 - P_{qe}(E_{\text{c.m.}} - \frac{\hbar^2 \Lambda}{2\mu R_b^2}, J = 0)], \tag{5}$$

where $\lambdabar^2 = \hbar^2/(2\mu E_{\text{c.m.}})$ is the reduced de Broglie wavelength, $\mu = m_0 A_1 A_2/(A_1 + A_2)$ is the reduced mass (m_0 is the nucleon mass), and at given bombarding energy $E_{\text{c.m.}}$ the summation is over the possible values of angular momentum J from $J = 0$ to the critical angular momentum $J = J_{cr}$. For values J greater than J_{cr}, the potential pocket in the nucleus-nucleus interaction potential vanishes and the capture is not occur. To calculate the critical angular momentum J_{cr} and the position R_b of the Coulomb barrier, we use the nucleus-nucleus interaction potential $V(R, J)$ of Ref. [7]. For the nuclear part of the nucleus-nucleus potential, the double-folding formalism with the Skyrme-type density-dependent effective nucleon-nucleon interaction is employed [7].

If one sets $R_b(J) \approx R_b$ in Eq. (5) for approximating the J-wave penetrability by the s-wave penetrability at a shifted energy, one obtains only the leading term in the series expansion in Λ. The next term in this expansion can be easily calculated in the same way as in Ref. [6] $[R_b(J) \approx R_b - \frac{\hbar^2 \Lambda}{\mu \alpha R_b^3}, V_b(J) \approx V_b + \frac{\hbar^2 \Lambda}{2\mu R_b^2} + \frac{\hbar^4 \Lambda^2}{2\mu^2 \alpha R_b^6}, \alpha = -\partial^2 V(R, J = 0)/\partial R^2|_{R=R_b} = \mu \omega_b^2, \omega_b = \omega_b(J = 0)$ is the curvature of the s-wave potential barrier with the height $V_b = V_b(J = 0) = V(R = R_b, J = 0)]$:

$$P_{cap}(E_{\text{c.m.}}, J) \approx P_{cap}(E_{\text{c.m.}} - \frac{\hbar^2 \Lambda}{2\mu R_b^2} - \frac{\hbar^4 \Lambda^2}{2\mu^2 \alpha R_b^6}, J = 0). \tag{6}$$

With this improved expression for the P_{cap}, we obtain

$$\sigma_{cap}(E_{\text{c.m.}}) = \pi \lambdabar^2 \sum_{J=0}^{J_{cr}} (2J+1)[1 - P_{qe}(E_{\text{c.m.}} - \frac{\hbar^2 \Lambda}{2\mu R_b^2}, J = 0)][1 - \frac{2\hbar^2 \Lambda}{\mu^2 \omega_b^2 R_b^4}]. \tag{7}$$

Converting the sum over J into an integral and changing variables to $E = E_{\text{c.m.}} - \frac{\hbar^2 \Lambda}{2\mu R_b^2}$ in Eq. (7), we obtain the following simple expression:

$$\sigma_{cap}(E_{\text{c.m.}}) = \frac{\pi R_b^2}{E_{\text{c.m.}}} \int_{E_{\text{c.m.}} - \frac{\hbar^2 \Lambda_{cr}}{2\mu R_b^2}}^{E_{\text{c.m.}}} dE[1 - d\sigma_{qe}(E)/d\sigma_{Ru}(E)][1 - \frac{4(E_{\text{c.m.}} - E)}{\mu \omega_b^2 R_b^2}], \tag{8}$$

which relates the capture cross section with quasielastic excitation function. Note that Λ is not a small parameter, there is a natural cutoff $\Lambda_{cr} = J_{cr}(J_{cr} + 1)$ in this parameter. Because of this cutoff, the second term $\frac{\hbar^2 \Lambda}{2\mu R_b^2}$ in Eq. (6) is always larger than the third one $\frac{\hbar^4 \Lambda^2}{2\mu^2 \alpha R_b^6}$ [6]. By using the experimental quasielastic probabilities $P_{qe}(E_{\text{c.m.}}, J = 0)$ and Eq. (8) one can obtain the capture cross sections.

For the systems with $Z_1 \times Z_2 < 2000$, the critical angular momentum J_{cr} is large enough and Eqs. (7) and (8) can be approximated with a good accuracy as:

$$\sigma_{cap}(E_{\text{c.m.}}) \approx \pi \lambdabar^2 \sum_{J=0}^{\infty} (2J+1)[1 - P_{qe}(E_{\text{c.m.}} - \frac{\hbar^2 \Lambda}{2\mu R_b^2}, J = 0)][1 - \frac{2\hbar^2 \Lambda}{\mu^2 \omega_b^2 R_b^4}] \tag{9}$$

and

$$\sigma_{cap}(E_{\text{c.m.}}) \approx \frac{\pi R_b^2}{E_{\text{c.m.}}} \int_0^{E_{\text{c.m.}}} dE[1 - d\sigma_{qe}(E)/d\sigma_{Ru}(E)][1 - \frac{4(E_{\text{c.m.}} - E)}{\mu \omega_b^2 R_b^2}]. \tag{10}$$

Following the procedure of Ref. [6] and using the extracted σ_{cap} and the experimental P_{qe}, one can find the average angular momentum

$$<J> = \frac{\pi R_b^2}{E_{\text{c.m.}} \sigma_{cap}(E_{\text{c.m.}})} \int_{E_{\text{c.m.}} - \frac{\hbar^2 \Lambda_{cr}}{2\mu R_b^2}}^{E_{\text{c.m.}}} dE[1 - d\sigma_{qe}(E)/d\sigma_{Ru}(E)][1 - \frac{5(E_{\text{c.m.}} - E)}{\mu \omega_b^2 R_b^2}]$$

$$\times [(\frac{2\mu R_b^2}{\hbar^2}(E_{\text{c.m.}} - E) + \frac{1}{4})^{1/2} - \frac{1}{2}] \tag{11}$$

and the second moment of the angular momentum

$$<J(J+1)> = \frac{2\pi \mu R_b^4}{\hbar^2 E_{\text{c.m.}} \sigma_{cap}(E_{\text{c.m.}})} \int_{E_{\text{c.m.}} - \frac{\hbar^2 \Lambda_{cr}}{2\mu R_b^2}}^{E_{\text{c.m.}}} dE[1 - d\sigma_{qe}(E)/d\sigma_{Ru}(E)][1 - \frac{6(E_{\text{c.m.}} - E)}{\mu \omega_b^2 R_b^2}]$$

$$\times [E_{\text{c.m.}} - E] \tag{12}$$

of the captured system.
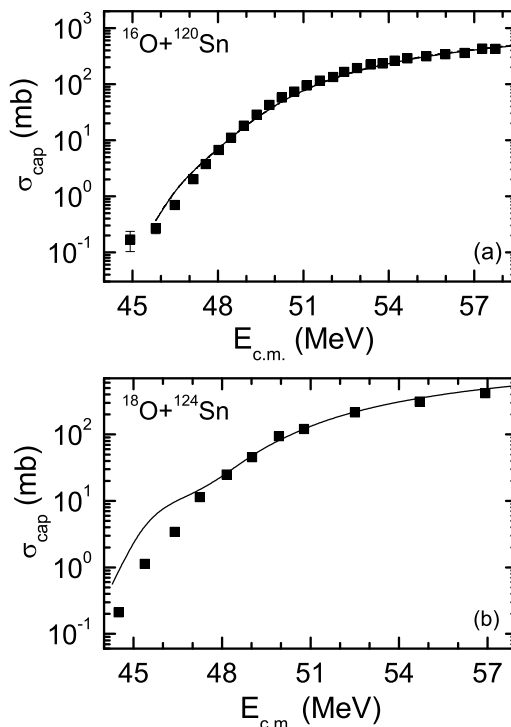
FIG. 1: The extracted capture cross sections for the reactions ^{16}O + ^{120}Sn (a) and ^{18}O + ^{124}Sn (b) by employing Eq. (8) (solid line) and Eq. (10) (dotted line). These lines are almost coincide. The used experimental quasielastic data are from Ref. [8]. The experimental capture (fusion) data (symbols) are from Refs. [8, 9].

III.   RESULTS OF CALCULATIONS

For the verification of our method of the extraction of σ_{cap}, firstly we compare the extracted capture cross sections with experimental one. In Figs. 1 and 2 one can see a good agreement between the extracted and directly measured capture cross sections for the reactions ^{16}O + ^{120}Sn, ^{18}O + ^{124}Sn, ^{16}O + ^{208}Pb, and ^{16}O + ^{144}Sm at energies above the Coulomb barrier. The results on the sub-barrier energy region are discussed later on. To extract the capture cross section, we use both Eq. (8) (solid lines) and Eq. (10) (dotted lines). The used values of critical angular momentum are J_{cr}=54, 56, 57, and 62 for the reactions ^{16}O + ^{120}Sn, ^{18}O + ^{124}Sn, ^{16}O + ^{144}Sm, and ^{16}O + ^{208}Pb, respectively. The difference between the results of Eqs. (8) and (10) is less than 5% at the highest energies. At low energies, Eqs. (8) and (10) lead to the same values of σ_{cap}. The factor $1 - \frac{4(E_{c.m.}-E)}{\mu\omega_b^2 R_b^2}$ in Eqs. (8) and (10) very weakly influences the results of the calculations for the systems and energies considered. Hence, one can say that for the relatively light systems the proposed method of extracting the capture cross section is model independent (particular, independent on the potential used).

One can see that the used formulas are suitable not only for almost spherical nuclei (Figs. 1 and 2), but also for the reactions with strongly deformed target- or projectile-nucleus (Figs. 3 and 4). The deformation effect is effectively contained in the experimental P_{qe}. $J_{cr} = 58, 68, 74$, and 76 for the reactions ^{16}O+^{154}Sm, ^{32}S+^{90}Zr, ^{32}S+^{96}Zr, and ^{20}Ne+^{208}Pb, respectively. The results obtained by employing the formula (10) are almost the same and not presented in Figs. 3 and 4.

For the reactions ^{16}O+^{154}Sm and ^{32}S+^{96}Zr, the extracted capture cross sections are shifted in energy by 1.7 and 1.9 MeV, respectively, with respect to the measured capture data. This could be the result of different energy calibrations in the experiments on the capture measurement and on the quasielastic scattering. Because of the lack of systematics in these energy shifts, their origin remains unclear and we adjust the Coulomb barriers in the extracted capture cross sections to the values following the experiments.

Note that the extracted and experimental capture cross sections deviate from each other in the reactions ^{16}O+^{208}Pb, ^{16}O+^{144}Sm, and ^{32}S+^{90}Zr at energies below the Coulomb barrier. Probably this deviation is a reason for the large discrepancies in the diffuseness parameter extracted from the analyses of the quasielastic scattering and fusion (capture) at deep sub-barrier energies. One of the possible reasons for the overestimation of the capture cross section from the quasielastic data at sub-barrier energies is the underestimation of the total reaction differential cross section
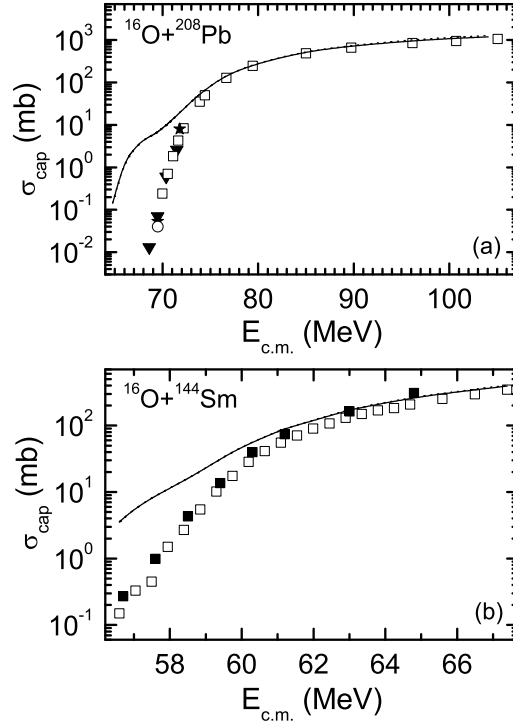
FIG. 2: The same as in Fig. 1, but for the reactions ^{16}O + ^{208}Pb(a),^{144}Sm(b). The used experimental quasielastic data are from Refs. [3, 4]. For the ^{16}O + ^{208}Pb reaction, the experimental capture (fusion) data are from Refs. [10] (open squares), [11] (open circles), [12] (closed stars), and [13] (closed triangles). For the ^{16}O + ^{144}Sm reaction, the experimental capture (fusion) data are from Refs. [14] (closed squares) and [15] (open squares).
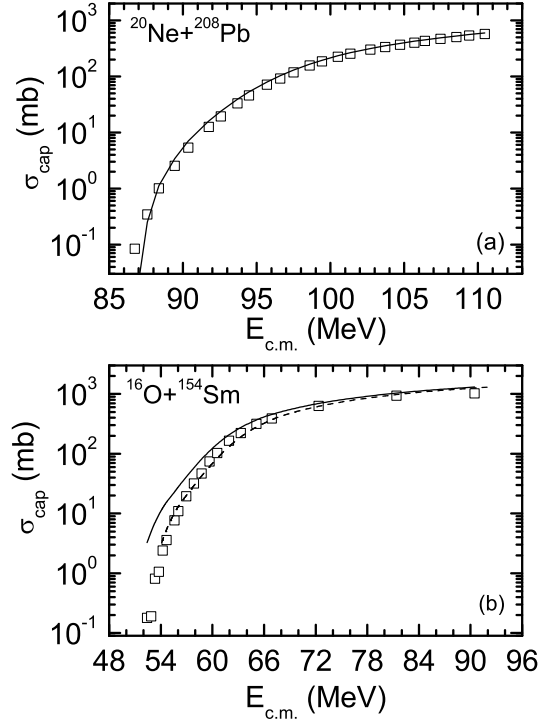

FIG. 3: The same as in Fig. 1, but for the reactions ^{20}Ne + ^{208}Pb and ^{16}O + ^{154}Sm. The used experimental quasielastic data are from Refs. [3, 16]. The experimental capture (fusion) data (symbols) are from Refs. [15, 16]. For the ^{16}O + ^{154}Sm reaction, the dashed line is obtained from the shift of the solid line by 1.7 MeV higher energies.
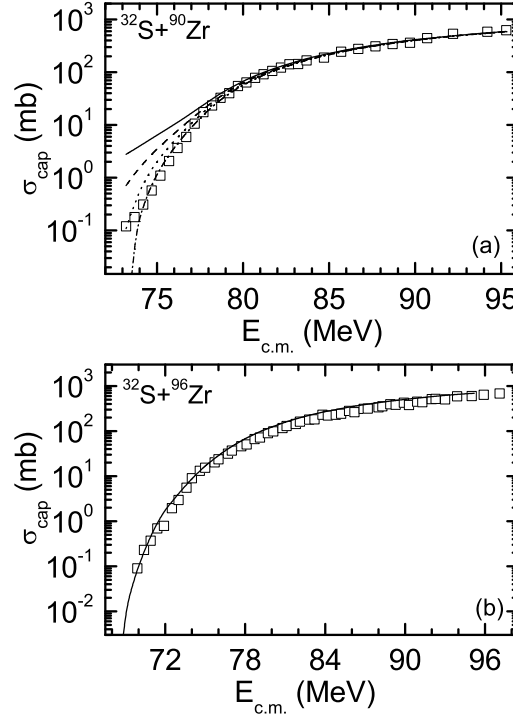
FIG. 4: The same as in Fig. 1, but for the reactions ^{32}S + ^{90}Zr (a) and ^{32}S + ^{96}Zr (b). For the ^{32}S+^{90}Zr reaction, we show the extracted capture cross sections, increasing the experimental P_{qe} by 1% (dashed line), 2% (dotted line), and 3% (dash-dotted line). The used experimental quasielastic data are from Ref. [17]. The experimental capture (fusion) data (symbols) are from Ref. [18]. For the ^{32}S + ^{96}Zr reaction, the energy scale for the extracted capture cross sections is adjusted to that of direct measurements.

taken as the Rutherford differential cross section. Indeed, for the ^{32}S+^{90}Zr reaction, the increase of P_{qe} within 2–3% is in order to obtain the agreement between the extracted and measured capture cross sections at the sub-barrier energies [Fig. 4(a)].

One can use Eq. (8) and available experimental quasielasic data [19] to predict the capture cross sections for the reactions ^{48}Ti,^{54}Cr,^{56}Fe,^{64}Ni,^{70}Zn + ^{208}Pb, using J_{cr} = 78, 74, 58, 51, 31, respectively. The extracted capture cross sections $\sigma_{cap}(E_{c.m.})$ as a function of $E_{c.m.}$ are presented in Fig. 5 (a). The formulas (8) and (10) give almost the same capture cross sections for reactions ^{48}Ti,^{54}Cr + ^{208}Pb at energies under consideration. Thus, for these systems, the values of J_{cr} are relatively large and the account of J_{cr} does not affect the results. However, for heavier systems with smaller J_{cr} (the smaller potential pockets in the nucleus-nucleus interaction potentials), the deviation between the results obtained with Eqs. (8) and (10) increases strongly with the factor $Z_1 \times Z_2$. The σ_{cap}, calculated with the finite value of critical angular momentum, decreases with increasing Coulomb repulsion in the system. One can try to check experimentally these predictions of $\sigma_{cap}(E_{c.m.})$ by the direct measurement of the capture cross sections. Note that the values of the extracted capture cross sections for the ^{48}Ti + ^{208}Pb system are close to those found in the experiments ^{50}Ti + ^{208}Pb [20, 21]. However, for the ^{64}Ni + ^{208}Pb system, there are strong deviations in the energy between the extracted and experimental [22] capture cross sections.

By using the extracted $\sigma_{cap}(E_{c.m.})$ and the sharp-cutoff approximation, one can determine the maximal angular momentum J_{max} in the captured system as a function of the bombarding energies:

$$J_{max} = [2\mu E_{c.m.}\sigma_{cap}(E_{c.m.})/(\pi\hbar^2)]^{1/2} - 1. \tag{13}$$

The extracted J_{max} for the cold fusion reactions are shown in Fig. 5(b). For the system ^{70}Zn + ^{208}Pb, the small depth of the potential pocket in the nucleus-nucleus interaction potential leads to the decrease of J_{max} by the factor about of 2.4 at highest energy considered (about of 17 MeV above the Coulomb barrier).

In the reactions with weakly bound nuclei one can extract the capture cross section by employing the conservation of the reaction flux [1, 23–25]

$$P_{cap}(E_{c.m.}, J = 0) = 1 - [P_{qe}(E_{c.m.}, J = 0) + P_{BU}(E_{c.m.}, J = 0)] \tag{14}$$

and the measured probabilities of the quasielastic scattering ($P_{qe}(E_{c.m.}, J = 0) = d\sigma_{qe}/d\sigma_{Ru}$) and of the breakup

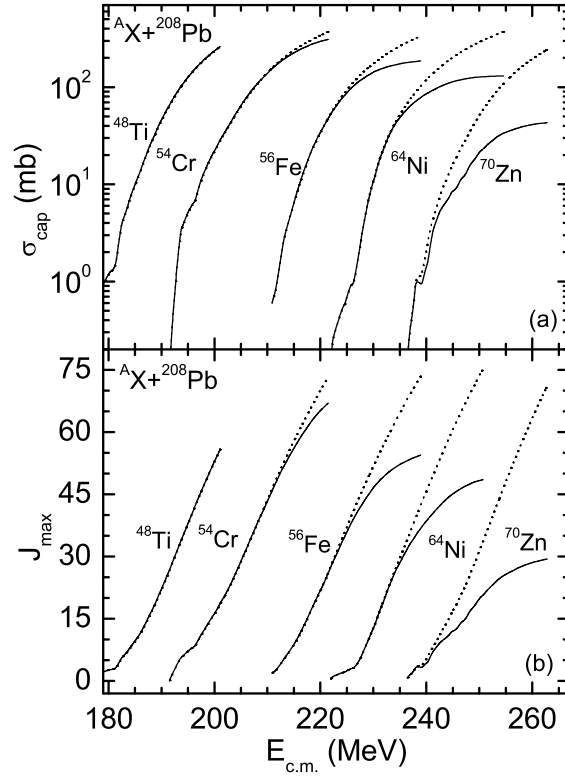FIG. 5: (a) The extracted capture cross sections employing Eq. (8) (solid line) and Eq. (10) (dotted line) for the reactions ^{48}Ti,^{54}Cr,^{56}Fe,^{64}Ni,^{70}Zn + ^{208}Pb. The used experimental quasielastic data are from Ref. [19]. (b) The extracted values of the maximal angular momenta vs. energy for the above mentioned reactions. The solid and dotted lines show the results of calculations of J_{max} by using the extracted capture cross sections calculated with Eqs. (8) and (10), respectively.

$(P_{BU}(E_{\text{c.m.}}, J = 0) = d\sigma_{BU}/d\sigma_{Ru})$ which are defined as the differential cross sections ratios between quasielastic scattering, breakup reaction and the Rutherford scattering at backward angle. As seen in Fig. 6, the extracted capture cross sections $\sigma_{cap}(E_{\text{c.m.}})$ (solid line) for the ^{6}Li+^{208}Pb reaction are rather close to those found in the direct measurements [26] at energies above the Coulomb barrier. It looks that at energies near and below the Coulomb barrier the extracted $\sigma_{cap}(E_{\text{c.m.}})$ deviates from the direct measurements. It is similarly possible to calculate the capture excitation function

$$\sigma_{cap}^{noBU}(E_{\text{c.m.}}) = \frac{\pi R_b^2}{E_{\text{c.m.}}} \int_{E_{\text{c.m.}} - \frac{\hbar^2 \Lambda_{cr}}{2\mu R_b^2}}^{E_{\text{c.m.}}} dE P_{cap}^{nBU}(E, J = 0)[1 - \frac{4(E_{\text{c.m.}} - E)}{\mu \omega_b^2 R_b^2}] \tag{15}$$

in the absence of the breakup process (Fig. 6, dotted line) by using the following formula for the capture probability in this case [25]:

$$P_{cap}^{nBU}(E_{\text{c.m.}}, J = 0) = 1 - \frac{P_{qe}(E_{\text{c.m.}}, J = 0)}{1 - P_{BU}(E_{\text{c.m.}}, J = 0)}. \tag{16}$$

By employing the measured excitation functions P_{qe} and P_{BU} at backward angle [24], Eqs. (8), (15), and the formula

$$< P_{BU} > (E_{\text{c.m.}}) = 1 - \frac{\sigma_{cap}(E_{\text{c.m.}})}{\sigma_{cap}^{noBU}(E_{\text{c.m.}})}, \tag{17}$$

we extract the mean breakup probability $< P_{BU} > (E_{\text{c.m.}})$ averaged over all partial waves J (Fig. 7). The value of $< P_{BU} >$ has a maximum at $E_{\text{c.m.}} - V_b \approx 4$ MeV ($< P_{BU} >$=0.26) and slightly (sharply) decreases with increasing (decreasing) $E_{\text{c.m.}}$. The experimental breakup excitation function at backward angle has the similar energy behavior [24]. By comparing the calculated capture cross sections in the absence of breakup and experimental capture (complete fusion) data, the opposite energy trend is found in Ref. [25], where $< P_{BU} >$ has a minimum at $E_{\text{c.m.}} - V_b \approx 2$ MeV

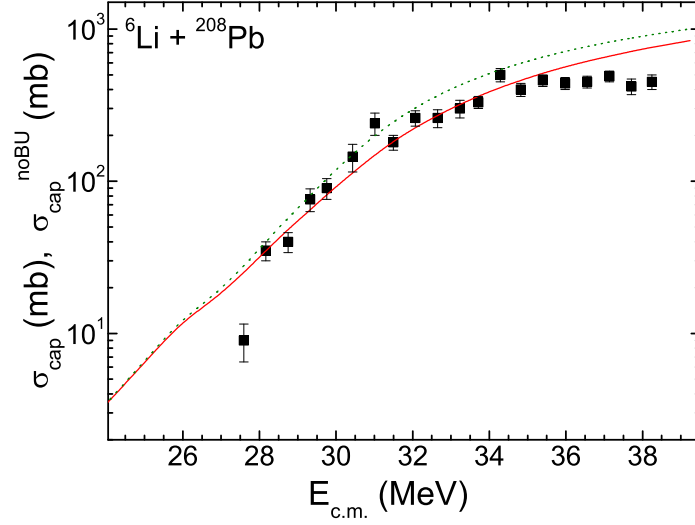FIG. 6: (Colour online) The extracted capture cross sections $\sigma_{cap}(E_{\mathrm{c.m.}})$ (solid line) and $\sigma_{cap}^{noBU}(E_{\mathrm{c.m.}})$ (dotted line) for the ^{6}Li+^{208}Pb reaction. The used experimental quasielastic and quasielastic plus breakup data are from Ref. [24]. The experimental capture cross sections (solid squares) are from Refs. [26]. The energy scale for the extracted capture cross sections is adjusted to that of direct measurements.
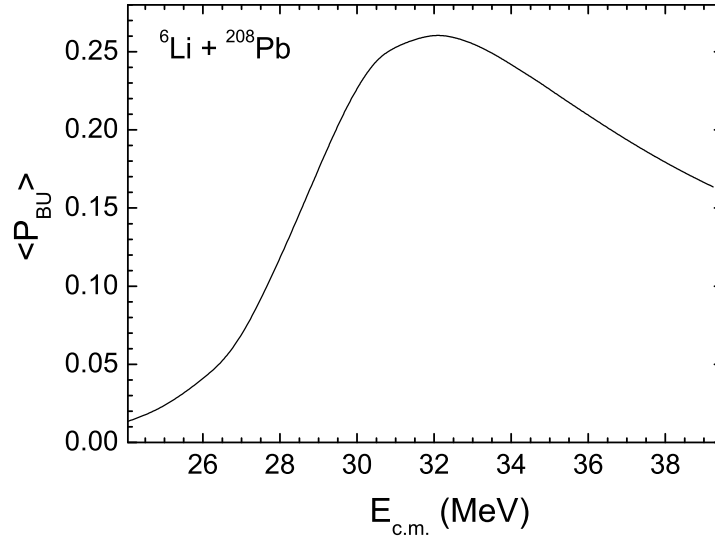

FIG. 7: The extracted mean breakup probability $< P_{BU} > (E_{\mathrm{c.m.}})$ [Eq. (14)] as a function of bombarding energy $E_{\mathrm{c.m.}}$ for the ^{6}Li+^{208}Pb reaction. The used experimental quasielastic and quasielastic plus breakup data are from Ref. [24].

($< P_{BU} >$=0.34) and globally increases in both sides from this minimum. It is also shown in Refs. [25, 27] that there are no systematic trends of breakup in the complete fusion reactions with the light projectiles ^{9}Be, ^{6,7,9}Li, and ^{6,8}He at near-barrier energies. Thus, by employing the experimental quasielastic backscattering, one can obtain the additional information about the breakup process. By using the Eqs. (11) and (12) and experimental P_{qe}, we extract $< J >$ and $< J^2 >$ of the captured system for the reactions ^{16}O + ^{154}Sm and ^{16}O + ^{208}Pb, respectively (Fig. 8). The agreements with the results of direct measurements of the $\gamma-$multiplicities in the corresponding complete fusion reactions are quite good. For the ^{16}O + ^{208}Pb reaction at sub-barrier energies, the difference between the extracted and experimental angular momenta is related with the deviation of the extracted capture excitation function from the experimental one (see Fig. 2). In Fig. 9 we present the predictions of $< J >$ for the reactions ^{16}O + ^{120}Sn and ^{32}S + ^{96}Zr.
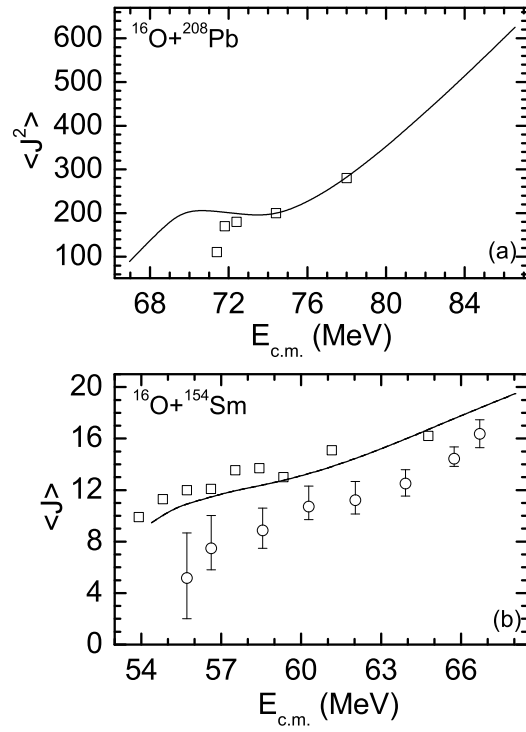
FIG. 8: The extracted $< J >$ and $< J^2 >$ for the reactions ^{16}O + ^{208}Pb (a) and ^{16}O + ^{154}Sm (b) by employing Eqs. (11) and (12). The used experimental quasielastic data are from Ref. [4]. The experimental data of $< J^2 >$ and $< J >$ are from Refs. [28] (open squares) and [29, 30] (open squares and circles), respectively.
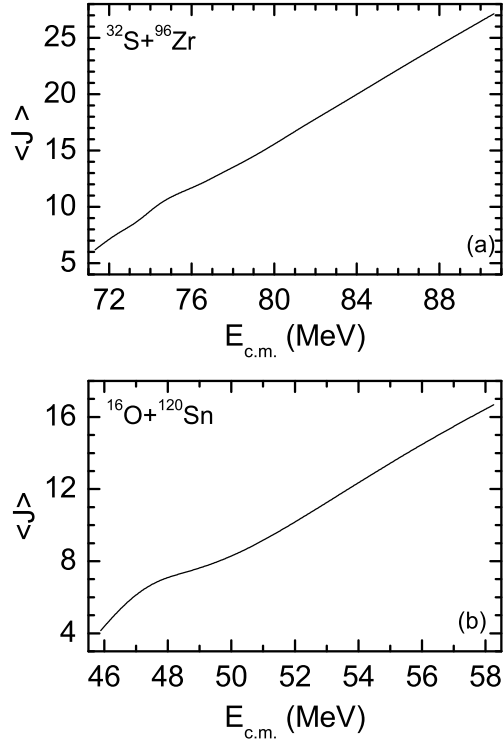

FIG. 9: The extracted $< J >$ for the reactions ^{32}S + ^{96}Zr (a) and ^{16}O + ^{120}Sn (b) by employing Eq. (11). The used experimental quasielastic data are from Refs. [8, 17].

IV. SUMMARY

We realized that the found relationship between the quasielastic excitation function and capture cross sections is working well, and the quasielastic technique could be an important and simple tool in the study of the capture (fusion) research, especially, in the cold and hot fusion reactions and in the breakup reactions at energies near and above the Coulomb barrier. Employing the quasielastic data, one can also extract the moments of the angular momentum of the captured system.

[1] L.F. Canto, P.R.S. Gomes, R. Donangelo, and M.S. Hussein, Phys. Rep. **424**, 1 (2006).
[2] V.V. Sargsyan, G.G. Adamian, N.V. Antonenko, W. Scheid, and H.Q. Zhang, Eur. Phys. J. A **49**, 19 (2013).
[3] H. Timmers, J.R. Leigh, M. Dasgupta, D.J. Hinde, R.C. Lemmon, J.C. Mein, C.R. Morton, J.O. Newton, and N. Rowley, Nucl. Phys. **A584**, 190 (1995); H. Timmers *et al.*, J. Phys. G **23**, 1175 (1997).
[4] H. Timmers, Ph.D. thesis, Australian National University (1996).
[5] H.Q. Zhang, F. Yang, C. Lin, Z. Liu, and Y. Hu, Phys. Rev. C **57**, R1047 (1998).
[6] A.B. Balantekin, A.J. DeWeerd, and S. Kuyucak, Phys. Rev. C **54**, 1853 (1996).
[7] G.G. Adamian, N.V. Antonenko, R.V. Jolos, S.P. Ivanova, O.I. Melnikova, Int. J. Mod. Phys. E **5**, 191 (1996); V.V. Sargsyan, G.G. Adamian, N.V. Antonenko, W. Scheid, and H.Q. Zhang, Phys. Phys. C **84**, 064614 (2011).
[8] S. Sinha, M.R. Pahlavani, R. Varma, R.K. Choudhury, B.K. Nayak, and A. Saxena, Phys. Rev. C **64**, 024607 (2001).
[9] P. Jacobs, Z. Fraenkel, G. Mamane, and L. Tserruya, Phys. Lett. B **175**, 271 (1986).
[10] C.R. Morton *et al.*, Phys. Rev. C **60**, 044608 (1999).
[11] Yu.Ts. Oganessian *et al.*, JINR Rapid Commun. **75**, 123 (1996).
[12] S.P. Tretyakova *et al.*, Nucl. Phys. **A734**, E33 (2004).
[13] M. Dasgupta *et al.*, Phys. Rev. Lett. **99**, 192701 (2007).
[14] D.E. DiGregorio *et al.*, Phys. Rev. C **39**, 516 (1989).
[15] J.R. Leigh *et al.*, Phys. Rev. C **52**, 3151 (1995).
[16] E. Piasecki *et al.*, Phys. Rev. C **85**, 054608 (2012).
[17] F. Yang, C.J. Lin, X.K. Wu, H.Q. Zhang, C.L. Zhang, P. Zhou, and Z.H. Liu, Phys. Rev. C **77**, 014601 (2008).
[18] H.Q. Zhang, C.J. Lin, F. Yang, H.M. Jia, X.X. Xu, Z.D. Wu, F. Jia, S.T. Zhang, Z.H. Liu, A. Richard, and C. Beck, Phys. Rev. C **82**, 054609 (2010).
[19] S. Mitsuoka, H. Ikezoe, K. Nishio, K. Tsuruta, S.C. Jeong, and Y. Watanabe, Phys. Rev. Lett. **99**, 182701 (2007).
[20] R.S. Naik, W. Loveland, P.H. Sprunger, A.M. Vinodkumar, D. Peterson, C.L. Jiang, S. Zhu, X. Tang, E.F. Moore, and P. Chowdhury, Phys. Rev. C **76**, 054604 (2007).
[21] H.-G. Clerc *et al.*, Nucl. Phys. **A419**, 571 (1984).
[22] R. Bock *et al.*, Nucl. Phys. **A388**, 334 (1982); J. Töke *et al.*, Nucl. Phys. **A440**, 327 (1985).
[23] H.M. Jia, C.J. Lin, H.Q. Zhang, Z.H. Liu, N. Yu, F. Yang, F. Jia, X.X. Xu, Z.D. Wu, S.T. Zhang, and C.L. Bai, Phys. Rev. C **82**, 027602 (2010).
[24] C.J. Lin *et al.*, Nucl. Phys. **A787**, 281c (2007).
[25] V.V. Sargsyan, G.G. Adamian, N.V. Antonenko, W. Scheid, and H.Q. Zhang, Phys. Rev. C **86**, 054610 (2012).
[26] Y.W. Wu, Z.H. Liu, C.J. Lin, H.Q. Zhang, M. Ruan, F. Yang, Z.C. Li, M. Trotta, and K. Hagino, Phys. Rev. C **68**, 044605 (2003).
[27] P.R.S. Gomes, J. Lubian, and L.F. Canto, Phys. Rev. C **79**, 027606 (2009); P.R.S. Gomes, R. Linares, J. Lubian, C.C. Lopes, E.N. Cardozo, B.H.F. Pereira, and I. Padron, Phys. Rev. C **84**, 014615 (2011).
[28] R. Vandenbosch, Annu. Rev. Nucl. Part. Sci. **42**, 447 (1992).
[29] S. Gil, R. Vandenbosch, A. Charlop, A. Garcia, D.D. Leach, S.J. Luke, and S. Kailas, Phys. Rev. C **43**, 701 (1991).
[30] R. Vandenbosch, B.B. Back, S. Gil, A. Lazzarini, and A. Ray, Phys. Rev. C **28**, 1161 (1983).